2001 European Control Conference (ECC)
Porto, Portugal, 4-7 September, 2001

ROBUST RST CONTROL FOR «BASSE-ISÈRE» RUN-OF-RIVER CASCADED HYDRO-ELECTRIC PLANTS

D. Dumur[(1)], A. Libaux[(2)], P. Boucher[(1)]

[(1)] **École Supérieure d'Électricité, Plateau de Moulon, F 91192 Gif-sur-Yvette cedex, France**
Fax: +33 (0)1 69 85 13 89
e-mail: didier.dumur@supelec.fr
[(2)] **EDF CIH FCC, F 73373 Le Bourget du Lac cedex, France**
Fax: +33 (0)4 79 60 63 89
e-mail: antoine.libaux@edf.fr

Keywords: Robust control, Identification, Pole placement design, Process control.

Abstract.

The design of run-of-river hydro-plant automation remains a challenge in combined terms of performance and security. This paper presents an innovative methodology, based on one hand on identification through available measurements, and on the other hand on a control structure including a local water level control added to a feed-forward action.
The water level controller, developed from the continuous-time robust pole placement structure of Ph. de Larminat, is examined here in a complete discrete-time framework, and requires only some direct manipulations of the assigned poles. This strategy leads to a very simple and efficient design, with easy to tune RST polynomial controllers, and is able to deal with the trade-offs between robustness, performance and noise sensitivity. Results of experimental application on the «Basse-Isère» cascade are finally presented.

1 Introduction

Unsuccessful attempts to improve automation of hydro-electric plants of the «Basse-Isère» have been made for many years, due to methodologies non adapted to this particular hydro cascade.
A more powerful solution is proposed here, which provides simple and efficient methods to ensure performance and security. This solution includes on one hand identification and modelling based on a transfer function approach rather than non linear Saint-Venant equations (which is the usual tool for river modelling and simulation), on the other hand an original control, combining a feed-forward action applied through the measured entering flow, and a complementary water level controller which compensates uncertainties of the feed-forward action around the nominal operating flow.

2 Modelling of the hydraulic installations

2.1 General description

The «Basse-Isère» cascade (between Grenoble and Valence, France) contains five river reaches and five 40/50 MW plants: Beauvoir, Saint-Hilaire, Pizançon, La Vanelle and Beaumont-Monteux, from upper to downstream side. River flow may vary from 70 to 3000 m^3/s, but automation is restricted to 900 m^3/s. Moreover, «La Bourne» river is a tributary of «Isère» and adds to the main flow, between Beauvoir and Saint Hilaire plants, inducing large perturbations.

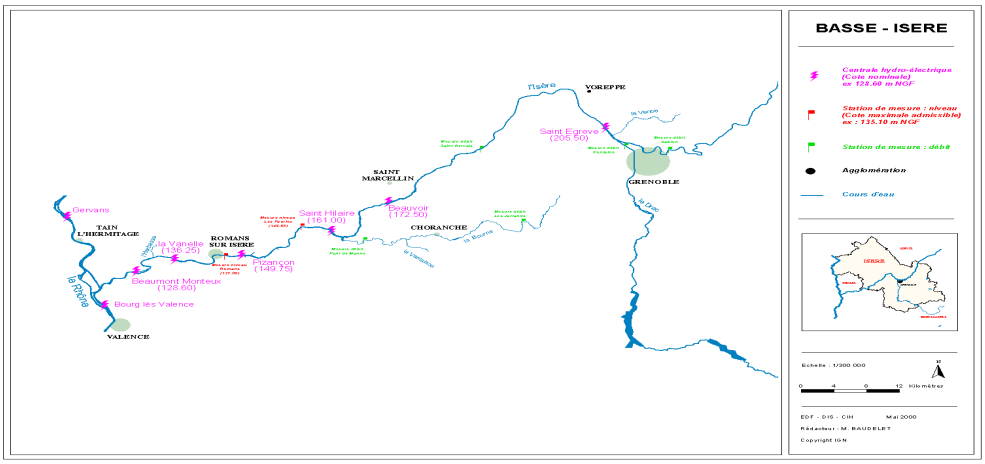

Figure 1: Geographical view of the «Basse-Isère» river and hydro-electric plants.

ISBN 978-3-9524173-6-2

Centralized operation and supervision is located in the P.S.H. (Hydraulic Supervisory Center) at Pizançon. Furthermore, two flow measurement stations are available upstream at Saint Gervais on the «Isère» and at Pont De Manne on «La Bourne». Figure 1 gives a global overview of the whole area.

The automation of this cascaded structure is particularly complex, due to the small capacities of the reaches, the frequent inflow variations, also flow constraints downstream on the «Rhône» river must be realized and three critical water level points located near dwelling and roads must be secured.

2.2 Identification

Open-loop identification of the system is performed for a sampling period of two minutes, with on site available measurements, that is plant total flows (upstream and downstream of the reach), and water level to control. A two inputs – one output transfer function (in case of one observed level) is determined by an optimisation least-squares method. The example shown below is the Beaumont-Monteux reach model, identified with two consecutive days measurements (6 and 7 January 1999). In Figure 2, measured level and simulated level are compared with a very good achievement.

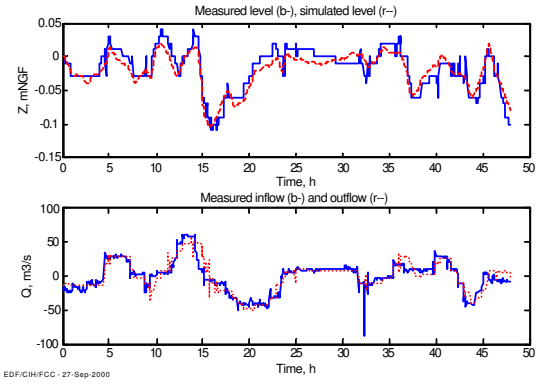

Figure 2: Comparison between measured and simulated level (Variations around the mean value of the two days measurements). Beaumont-Monteux.

In this case, and on the basis of discrete time transfer functions similar to the continuous ones described in [2], the identified models are:

- Between outflow (m^3/s) and water level (cm):

$$H_{11}(q^{-1}) = \frac{-5.343\ 10^{-4} q^{-2} + 4.59\ 10^{-4} q^{-3}}{1 - 1.468\ q^{-1} + 0.505\ q^{-2} - 0.0368\ q^{-3}} \qquad (1)$$

- Between inflow (m^3/s) and water level (cm):

$$H_{21}(q^{-1}) = \frac{3.075\ 10^{-5} q^{-4} - 2.661\ 10^{-5} q^{-5}}{1 + a_1 q^{-1} + a_2 q^{-2} + a_3 q^{-3} + a_4 q^{-4} + a_5 q^{-5}} \qquad (2)$$

with : $a_1 = -3.267 \quad a_2 = 4.168 \quad a_3 = -2.597$
$a_4 = 0.7892 \quad a_5 = -0.09332$

This technique is repeated over a full year, in order to determine the significant models for the whole flow range, then elaborate a mean model useful for the simulation described in Section 4. The engineering cost of such a method is obviously deeply smaller than a free-surface numerical model approach with two more significant advantages: firstly it gives knowledge of the process at all flows, even in flood events in particular, then a check-up can be done periodically if necessary.
Another result, useful for the operator, is to put in a prominent position the better knowledge of the error on the turbined or spilled plant flow. This error between the flow setting-point delivered by the control process or by the operator and the turbined flow is identified under the following linear form:

$$Q_{\text{real}} = a\, Q_{\text{setpoint}} + b \qquad (3)$$

In the case of Beaumont-Monteux shown here, the linear correction determined on La Vanelle (upstream) plant flow is 0.9, which means that the real entrance flow delivered by La Vanelle is in fact 10% smaller than the operating flow.

For the RST design phase, the previous transfer functions will be simplified, with only an integrative term and appropriate delays, considering that the robustness of the local controller is able to counteract parametric errors.

2.3 Design model

Considering two cascaded reaches, one upstream, *XX*, the other *YY* downstream, and neglecting wave propagation and complex phenomena, the behaviour of the *YY* reach can be described through the following differential equation [2, 6]:

$$S_{YY} \frac{dZ_{YY}(t)}{dt} = Q_{XX}(t - \tau_{XX->YY}) - Q_{YY}(t - \tau_{YY}) + q_a(t - \tau_a) \qquad (4)$$

With: t : time, in sec, T_e : sampling period, in sec (2 min for this application),
S_{YY} : water surface of reach *YY*, in m^2 ,
Z_{YY} : water level of reach *YY* to be controlled, in mNGF ,
$Q_{XX}(t - \tau_{XX->YY})$: inflow from upstream reach *XX*, in m^3/s ,
$\tau_{XX->YY}$: retention delay time due to propagation from upstream reach *XX* up to the level measurement at the plant of reach *YY*,
$Q_{YY}(t - \tau_{YY})$: reach *YY* controlled outflow, in m^3/s ,
τ_{YY} : about one sampling period maximum if the measured water level at the plant is the controlled level,
$q_a(t - \tau_a)$: if necessary, complementary flow of a tributary with the corresponding delay time up to the plant of reach *YY*, in m^3/s (will be omitted in further developments).

In a global way, a reach is an integrative system with delay times as represented on Figure 3. From the previous notations, the discrete time transfer function between the controlled outflow and the water level, used for the controller design:

$$H_1(q^{-1}) = \frac{Z_{YY}(q^{-1})}{Q_{YY}(q^{-1})} = \frac{T_e\ q^{-2}}{S_{YY}\ (1-q^{-1})} \tag{5}$$

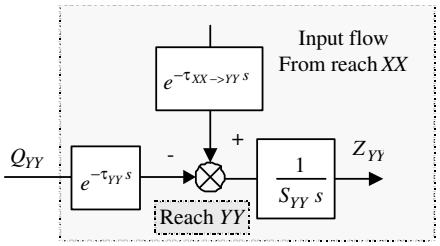

Figure 3: Block diagram of a reach.

3 Global control strategy

With the results of the previous part, and including the feed-forward action applied through the measured incoming flow and the water level controller, the control loop of reach *YY* is given on Figure 4. It must be noticed that the five reaches are cascaded, the outflow of one reach being the inflow of the following.

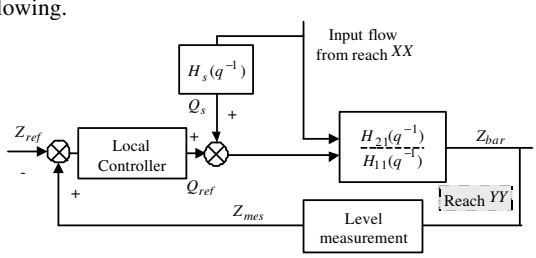

Figure 4: Water level control with feed-forward action.

3.1 Feed-forward action

This action, classical in river control, is imposed by time propagation and corresponds to the main flow action. This structure is realized in such a way that the filtered delayed inflow Q_s is added to the flow required by the controller Q_{ref}, in order to almost instantaneously compensate the influence of upstream overflows. According to strategies developed in [2], the transfer function of this feed-forward action has been chosen as a well-damped second order term including a delay time:

$$H_s(q^{-1}) = \frac{(1-K_{sYY})^2}{(1-K_{sYY}\,q^{-1})^2}\,q^{-\tau_{sYY}/T_e} \tag{6}$$

with: $\tau_{sYY} = \frac{\tau_{XX\to YY}}{3}$ and $K_{sYY} = e^{-\frac{3T_e}{\tau_{XX\to YY}}}$.

This tuning, tested in simulation, provides the best results in terms of smoothness of the anticipation and compensation of overflows.

3.2 Robust pole placement design

Because of small storage capacities decreasing from upstream to downstream, a more efficient control than PID is necessary. As previously mentioned, the water level local controller is based on the continuous-time robust pole placement structure of Ph. de Larminat [3], but presented here in an original discrete-time framework. The design methodology must provide at the end the polynomial controller under the classical RST form [5], as stated on Figure 5.

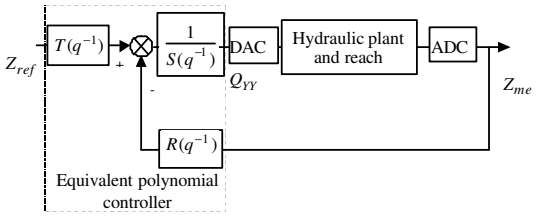

Figure 5: Equivalent polynomial controller.

Generalities. Consider a system modelled by an input/output discrete-time transfer function:

$$H(q) = \frac{y(t)}{u(t)} = \frac{B(q)}{A(q)} = \\ = \frac{b_0 + b_1\,q + \cdots + b_m\,q^m}{1 + a_1\,q + \cdots + a_n\,q^n} \quad \text{with}: \quad n > m \tag{7}$$

Where q corresponds to the forward shift operator, $u(t)$ and $y(t)$ to the input and output of the system. Considering the scheme of Figure 5, this transfer function characterises the three blocks {DAC, plant, ADC}, and corresponds for the application to $H_1(q)$ as defined by Equation (5).

According to Figure 5, and with the previous notation of Equation (7), the closed loop transfer function is given by:

$$H_{bf}(q) = \frac{T(q)B(q)}{A(q)\,S(q) + B(q)\,R(q)} \tag{8}$$

From this, the well-known principle of pole placement design consists in solving a Bezout identity:

$$A(q)\,S(q) + B(q)\,R(q) = C(q) \tag{9}$$

to obtain the unknown polynomials of the controller $R(q)$ and $S(q)$, with the a priori knowledge of the $C(q)$ polynomial. The solution is unique if the following regularity condition is fulfilled:

$$\text{degree}(A) + \text{degree}(B) \geq \text{degree}(C)$$

The fundamental methodological problem lies in determining the assigned closed loop poles in order to deal with the trade-offs between robustness, performances and noise sensitivity. Many authors were concerned with this problem [1, 4], the proposed approach here requires only some direct manipulations of the assigned poles to define the $C(q)$

polynomial in an equivalent way as with the LTR principle, but without the need for state space representation or Kalman formalism. Consider thus the following decomposition:

$$C(q) = F(q)P(q) \tag{10}$$

where $P(q)$ is the control polynomial, of degree n, with $P(1) = B(1)$, defining the control poles, and $F(q)$ is the filter normalized polynomial, of degree $n+1$, defining the observer poles.

Strategy for the control poles assignment. The $P(q)$ polynomial is elaborated looking at the roots of $B(q)$ and with the definition of a first design parameter T_c, the control horizon. The following four steps must be considered, as summarized on Figure 6:

- **i.** Unstable roots of $B(q)$ (outside the unit circle) are moved to their inverse $(a \to b)$,
- **ii.** Roots of $B(q)$ outside the circle defined by the points $\exp(-T_e/T_c)$ and 1 are projected on this circle $(b \to c)$,
- **iii.** $(n-m)$ zeros are added at location $\exp(-T_e/T_c)$ (d),
- **iv.** Normalisation.

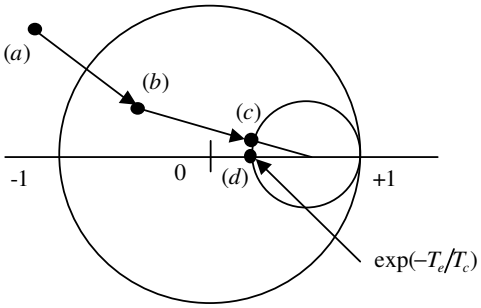

Figure 6: Design steps of the control polynomial.

Strategy for the filtering poles assignment. The $F(q)$ polynomial is elaborated looking at the roots of $A(q)$ and with the definition of a second design parameter T_o, the filter horizon. The following four steps must be considered, as summarised on Figure 7:

- **i.** Unstable roots of $A(q)$ (outside the unit circle) are moved to their inverse $(a \to b)$,
- **ii.** Roots of $A(q)$ outside the circle $C[0, \exp(-T_e/T_o)]$ are projected on this circle $(b \to c, f \to g)$,
- **iii.** Additional root at location $-\exp(-T_e/T_o)$ (d),
- **iv.** Normalisation.

Integral controller synthesis. The design of a controller including an integral action can be achieved with the following particular choice of the $R(q)$ and $S(q)$ polynomials:

$$S(q) = (q-1)S'(q) \qquad R(q) = T_e R'(q) \tag{11}$$

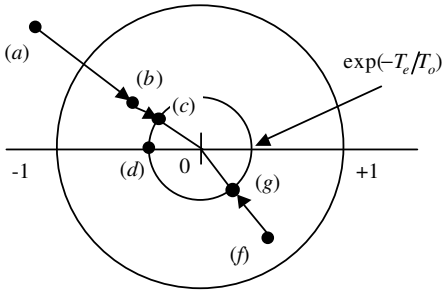

Figure 7: Design steps of the filter polynomial.

The remaining unknown factors being solution of the modified bezout equation:

$$A(q)(q-1)S'(q) + B(q)\,T_e\,R'(q) = C(q) \tag{12}$$

To conclude this synthesis, the $T(q)$ prefilter is chosen equal to $F(q)$. With the synthesis performed on the design model $H_1(q^{-1})$, the degrees of the three polynomials are:

$$\begin{aligned} &\text{degree}\left[R(q^{-1})\right] = \text{degree}\left[S(q^{-1})\right] = 3 \\ &\text{degree}\left[T(q^{-1})\right] = 2 \end{aligned} \tag{13}$$

Choice of the tuning parameters. The robust pole placement strategy requires the definition of two tuning parameters, the control horizon T_c, generally chosen near the sampling period value T_e, and the filter horizon T_o, generally chosen near the desired response time. The following remarks enable a more accurate tuning. Increasing T_o improves the phase and gain margins, and particularly the delay margin. However, regulation performance is damaged. Decreasing T_c improves the margins, particularly the gain margin, and to a lesser degree the delay margin and the regulation performance. However, the control signal becomes more sensitive to measurement noise.

To illustrate these 'rules', Figure 8 presents variations of the gain, phase, modulus and delay margins as function of the two tuning parameters, for the reach of Pizançon.

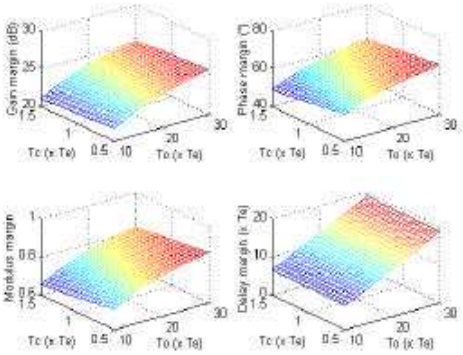

Figure 8: Tuning parameters influence on the stability and robustness margins – Reach of Pizançon.

4 Simulation results

Based on the reach models previously described and identified, but also including physical non-linearities (saturation, rate limitation, quantisation of measurements…) and more complex structures of the hydraulic part, a complete simulator of the cascaded architecture has been developed with Matlab/Simulink™ software. This simulator first of all aims at testing the performance of the designed controllers and feed-forward actions, but can also be considered as a useful tool for persons in charge of the complete implementation and supervision.

In this simulator, tests of performance are available for different kinds of inflows measured at the Saint Gervais and Pont De Manne stations. A typical scenario considered here corresponds to a real measured rising period, 20-24 February 1999.

The aim of the control strategy is to maintain the water levels at their nominal values (see Table 1 in Appendix) for the three reaches without critical points, and to secure the two critical locations, Les Fauries (between Saint Hilaire and Pizançon plants) and Romans (between Pizançon and La Vanelle plants) by implementing an adequate plant set-point profile.

With the tuning parameters of Table 1 in Appendix, the frequency features of the five controlled loops are given on Figure 9, showing the stability and robustness of the controlled system.

Beauvoir
Gain margin : 12.07 dB
Phase margin : 49.16 degrés
Bandwidth : 0.00089 rad/s
Delay margin : 8 *Te
Modulus margin : 0.66

Saint Hilaire
Gain margin : 13.3 dB
Phase margin : 51.85 degrés
Bandwidth : 0.00076 rad/s
Delay margin : 9.9 *Te
Modulus margin : 0.7

Pizançon
Gain margin : 11.81 dB
Phase margin : 47.61 degrés
Bandwidth : 0.00084 rad/s
Delay margin : 8.2 *Te
Modulus margin : 0.65

La Vanelle
Gain margin : 12.07 dB
Phase margin : 49.16 degrés
Bandwidth : 0.00089 rad/s
Delay margin : 8 *Te
Modulus margin : 0.66

Beaumont-Monteux
Gain margin : 9.83 dB
Phase margin : 47.12 degrés
Bandwidth : 0.0015 rad/s
Delay margin : 4.6 *Te
Modulus margin : 0.62

SIM-BI 1.0a (c) EDF CIH FCC - 20-Sep-2000

Figure 9: Frequency features of the five controlled loops.

Figures 10 and 11 show the resulting water levels, and outflows and feed-forward actions of the five reaches, and the two critical locations water levels. It is important to note on Figure 10 that the water levels are maintained at their nominal values with only a few centimetres fluctuations, even with important inflows. This performance proves the interest of the combined robust feedback control (for robustness of the cascaded loops towards parametric disturbances or neglected dynamics) and the feed-forward action (for an efficient compensation of upstream overflows). The necessity of the feed-forward term is shown on Figure 11, where important variations of the inflow are directly taken into account by this action.

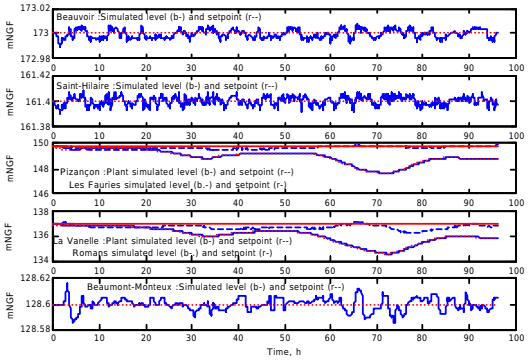

Figure 10: Water level of the five reaches, including two critical points.

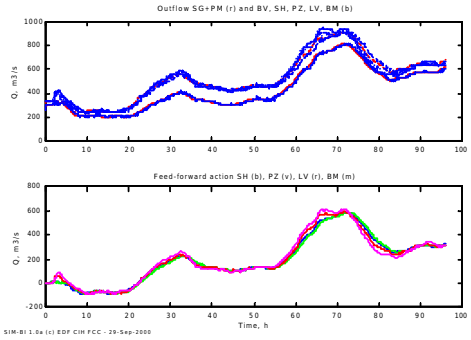

Figure 11: Outflow and feed-forward action of the five reaches.

5 Experimental results

The proposed solution has been progressively implemented on site since the beginning of summer 2000, from downstream to upstream, starting first with the reach of Beaumont-Monteux. For brevity, only two reaches are presented below, Beaumont-Monteux and La Vanelle. Figures 12 and 13 show the water levels of these two reaches measured on the 2 September 2000, together with the corresponding outflows. These results completely agree with the behaviour obtained in simulation and prove the global performance of the proposed strategy.

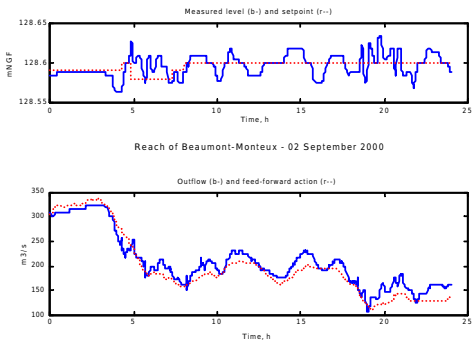

Figure 12: Measured plant level and critical location levels and outflow – Beaumont-Monteux.

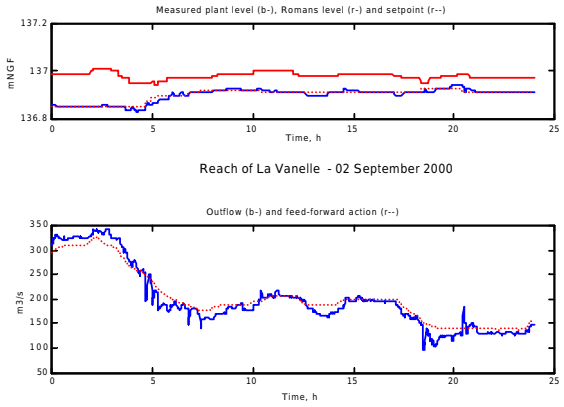

Figure 13: Measured plant level and critical location levels and outflow – La Vanelle.

6 Conclusion

This paper presents an efficient methodology for run-of-river hydro-electric plant operation, fully based on available measurements and identification technique.

A lot of unsuccessful attempts have been performed in the past years with PID controllers on the «Basse-Isère» cascade, always introducing amplification of instability from upstream to downstream (this phenomenon has also been detected through simulation).

That is the reason why the developed original robust RST control law, coupled to a classical feed-forward action with carefully elaborated tuning fitting the feedback objectives, proves to be a powerful structure compared to previous strategies for such hydraulic systems.

The simulation results of Section 4 show a confident behaviour of the automated system (in terms of stability, robustness and reliability), based on simple algorithms, similar for all reaches, and provides easy to use and comprehensive tools.

Moreover, experimental results achieved for five months now enforce the methodology, validate the simulation, and stress the performance of the proposed solution.

7 References

[1] K. Aström, B. Wittenmark. "Computer controlled systems, theory and design", *Prentice Hall*, (1990).

[2] B. Cuno, S. Theobald. "The relationship between control requirements, process complexity and modelling effort in the design of river control systems", *IMACS Journal, Mathematics and Computer in Simulation*, (1997).

[3] Ph. De Larminat, S. Puren. "Robust Pole Placement Design Via the LTR Approach", *Proceedings of the 14th IFAC World Congress*, Beijing, July, (1999).

[4] I.D. Landau. "Identification et commande des systèmes", *2nd edition, Hermès*, (1993).

[5] R. Longchamp. "Commande Numérique de Systèmes Dynamiques", *Presses Polytechniques et Universitaires Romandes*, (1995).

[6] J. Schuurmans, A.J. Clemmens. "Modelling of Irrigation and Drainage Canals for Controller Design", *Journal of Irrigation and Drainage Engineering*, November/December, (1999).

8 Appendix

	Beauvoir	Saint Hilaire	Pizançon	La Vanelle	Beaumont-Monteux
Reach water surface	$1.269\ 10^6\ m^2$	$1.189\ 10^6\ m^2$	$1.856\ 10^6\ m^2$	$1.240\ 10^6\ m^2$	$0.669\ 10^6\ m^2$
Delay time upstream → downstream reach	20 min	20 min	30 min	25 min	20 min
Delay time critical location → downstream reach barrage			20 min	15 min	
Barrage nominal level	173 m NGF	161.4 m NGF	149.75 mNGF	137 m NGF	128.6 m NGF
'Critical' location maximum water level			149.8 m NGF	137 m NGF	
Control horizon T_c	240 sec	240 sec	300 sec	240 sec	108 sec
Filter horizon T_o	1440 sec	1440 sec	1800 sec	1440 sec	840 sec

Table 1: Main features of the five reaches and tuning parameters of the robust pole placement RST controllers.